

Design and Investigation of a Photocatalytic Setup for Efficient Biotransformations Within Recombinant Cyanobacteria in Continuous Flow

Alessia Valotta,^{*,[a]} Lenny Malihan-Yap,^[b] Kerstin Hinteregger,^[a] Robert Kourist,^[b, c] and Heidrun Gruber-Woelfler^{*,[a]}

Photo- and biocatalysis show many advantages as more sustainable solutions for the production of fine chemicals. In an effort to combine the benefits and the knowledge of both these areas, a continuous photobiocatalytic setup was designed and optimized to carry out whole-cell biotransformations within cells of the cyanobacterium *Synechocystis* sp. PCC 6803 expressing the gene of the ene-reductase YqjM from *B. subtilis*. The effect of the light intensity and flow rate on the specific activity in the stereoselective reduction of 2-methyl maleimide

was investigated via a design-of-experiments approach. The cell density in the setup was further increased at the optimal operating conditions without loss in specific activity, demonstrating that the higher surface area/volume ratio in the coil reactor improved the illumination efficiency of the process. Furthermore, different reactor designs were compared, proving that the presented approach was the most cost- and time-effective solution for intensifying photobiotransformations within cyanobacterial cells.

Introduction

With an increasing need for more sustainable alternatives to traditional chemical processes, photo- and biocatalysis have arisen in recent years as possible ways to speed up reactions while keeping the amount of waste and resources low. Photocatalysis has significantly been used to overcome some problems connected with traditional catalysis, namely low activity, extreme reaction conditions, and safety concerns.^[1,2] The same can be applied to biocatalysis, which has been praised for its mild reaction conditions, high selectivity, and low environmental impact.^[3,4] Therefore, combining these two emerging sciences poses great advantages for a more efficient and sustainable production of fine chemicals, in line with the proposed principles of green chemistry.^[5,6] Especially in recent years, great advances have been achieved to study light-driven biotransformations and discover new photoenzymes.^[7-9] While


the study of the photoactive enzymes is still in its early stages, great interest has been devoted to study the photocatalytic regeneration of cofactors or cosubstrates, especially for biocatalytic redox reactions.^[7,9] Oxidoreductases, which catalyze a wide plethora of redox reactions, have been very attractive for industrial applications due to their high versatility and importance for organic synthesis.^[10,11] Despite their high selectivity and activity under mild conditions, oxidoreductases have the disadvantage of depending on expensive cofactors [e.g., nicotinamide adenine dinucleotide phosphate (NADPH) and nicotinamide adenine dinucleotide (NADH)] and exhibiting instability outside living cells.^[10] To overcome these issues, one of the proposed strategies for cofactor regeneration was to express oxidoreductases inside host cells such as *E. coli* to be used in whole-cell biocatalysis. However, the usage of heterotrophic host cells requires the addition of further cosubstrates (such as glucose) in stoichiometric amounts to fuel their metabolism, resulting in a poor atom economy and increasing environmental (E) factor.^[12,13] As a solution, the utilization of photoautotrophic microorganisms, such as cyanobacteria, has been suggested. In fact, coupling the cells' innate photosynthetic water splitting and reducing power for cofactor regeneration makes it possible to efficiently fuel a wide range of redox reactions with excellent efficiency and high reaction rates.^[14-17] This results in a more sustainable process, not only due to its high atom efficiency, but also because cyanobacteria capture CO₂ to convert it into biomass or useful compounds, and are active under visible light, which is largely available and can be considered a low-cost reagent.^[17]


Despite these advantages, the industrial application of light-driven (bio)transformations in cyanobacteria are limited due to scale-up difficulties.^[5] The main limiting factor in this regard is the illumination efficiency and light availability, especially when using an external light source and large tank reactors. To make

[a] A. Valotta, K. Hinteregger, Prof. Dr. H. Gruber-Woelfler
Institute of Process and Particle Engineering
Graz University of Technology
Inffeldgasse 13, 8010 Graz (Austria)
E-mail: valotta@tugraz.at
woelfler@tugraz.at

[b] Dr. L. Malihan-Yap, Prof. Dr. R. Kourist
Institute of Molecular Biotechnology
Graz University of Technology
Petersgasse 14, 8010 Graz (Austria)

[c] Prof. Dr. R. Kourist
ACIB GmbH
Krenngasse 37, 8010 Graz (Austria)

 Supporting information for this article is available on the WWW under <https://doi.org/10.1002/cssc.202201468>

 © 2022 The Authors. ChemSusChem published by Wiley-VCH GmbH. This is an open access article under the terms of the Creative Commons Attribution Non-Commercial License, which permits use, distribution and reproduction in any medium, provided the original work is properly cited and is not used for commercial purposes.

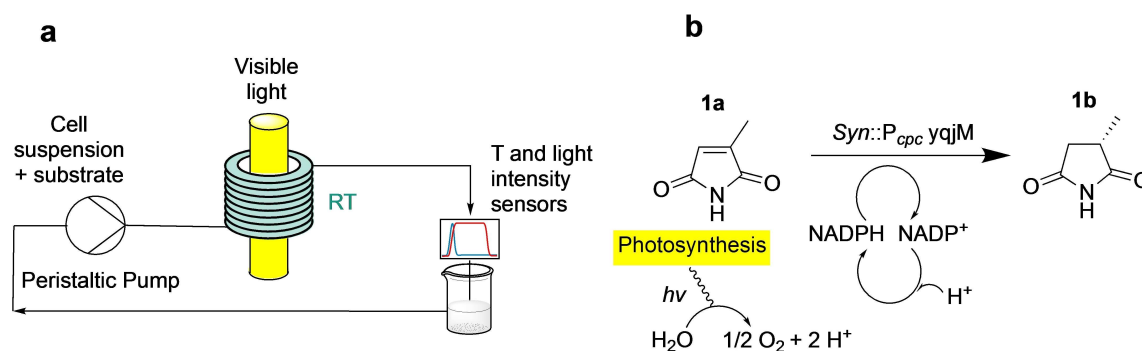
such reactions industrially competitive, it would be necessary to design photobioreactors with a high surface area/volume (S/V) ratio and optimal light distribution to allow short light penetration distances between the light source and the reaction medium.^[18] This is important considering that the cells absorb visible light and tend to self-shadow each other, especially at higher cell densities, limiting productivity and making scale-up more problematic.^[5]

To overcome these issues, photocatalysis in continuous flow could be a solution. Due to the small internal dimensions and the high S/V ratio of meso- [internal diameter (ID) > 1 mm] and microreactors (ID < 1 mm), flow reactors allow for more uniform light irradiation and shorter light penetration paths, thereby reducing the extent of dark areas in the reactor. The high S/V ratio also determines better mass transfer and mixing inside the reactor, which results in highly selective reactions and reduced byproduct formation.^[19,20] Moreover, the irradiation time can be easily adjusted by adapting the flow rate and the reactor length, therefore avoiding under- or over-irradiation of the reaction medium.^[18] Typical flow reactors, such as microchip, coil, and packed bed reactors have been implemented independently in photo-^[2,19–21] and biocatalytic processes^[22–25] with excellent results in terms of productivity and catalyst stability. However, despite the numerous benefits, there is still little work on photobiotransformations in flow for organic synthesis. So far, continuous photobioreactors have been used mostly for fermentative production of biomass, building blocks (such as isopropanol or ethanol), biofuels, isoprenoids, and also for the production of hydrogen.^[18,26,27] The utilization of recombinant resting cells has been mostly limited to small-scale batch applications; however, some novel reactor concepts have been proposed in recent works. A glass capillary reactor approach has already been investigated in literature,^[28,29] where a mixed culture containing *Synechocystis* sp. PCC 6803 (hereafter *Synechocystis* or Syn) cells have been immobilized in a biofilm on the reactor walls. Despite the promising long-term stability, high activity, and biocatalyst loading achieved, the system lacked enough space-time-yield (STY) since only 1 mM of the substrate was fed. Moreover, the immobilization of the biofilm occurred over long periods of time (over 37 days). In another work, a bubble column reactor (BCR) with an internal

illumination approach via wireless light emitters (WLE) has been implemented.^[5] Despite the promising results in terms of high reaction rates and specific activities, it was still limited in its scale-up by the cell density and possible oxygen accumulation. Scale-up also revealed to be an issue in another recent work, where a 2 L stirred tank photoreactor has been tested for the Baeyer-Villiger oxidation of cyclohexanone catalyzed by Syn harboring the Baeyer-Villiger Monooxygenase (BVMO) gene from *Acidovorax* sp. CHX100.^[30] Here, despite the high activities detected on 1 mL batch scale, when scaling up to 2 L more than half of the activity was lost and the substrate could not be completely converted, causing waste formation and lower productivity. This was most probably due to uneven light distribution within the stirred tank.

In this work, we exploit the benefits and the existing knowledge of flow photochemistry by using a helical coil reactor for photobiocatalytic ene-reduction reactions inside recombinant cyanobacteria cells in suspension. This reactor geometry has been widely used in flow photocatalysis due to its ease of assembly, implementation and scale-up.^[21] The coil reactor used in this work consists of a food-grade polyvinyl chloride (PVC) coil wrapped around a visible light source, as shown in Scheme 1a. The small internal diameter (2 mm) of the coil allows for a more homogeneous light distribution than in batch due to the smaller diffusion path of light. PVC was chosen as a highly transparent and easy-to-shape material, which also proved to be compatible with the cells. The setup was also designed to have an easy construction and adjustment due to the utilization of 3D printed tube holders, which can be used to regulate the light intensity at the reactor wall by simply adjusting the distance from the light source. To the best of our knowledge, this is the first time this reactor type has been used in a continuous photobiocatalytic application in cyanobacteria.

The chosen model reaction is shown in Scheme 1b. *Synechocystis* harboring the YqjM gene from *Bacillus subtilis* catalyzes the ene-reduction of 2-methylmaleimide (**1a**) to 2-methylsuccinimide (**1b**). The reaction consumes NADPH as a cofactor, which is converted to NADP⁺ as a result of the photosynthesis occurring in the thylakoid membrane of cyanobacteria, and therefore no further cofactor regeneration system is needed. The reaction has been chosen due to its high



Scheme 1. (a) Scheme of the reaction setup, including the measurement points for the used temperature and light sensors. (b) Scheme of the investigated model reaction.

stereoselectivity and specific activity, as it has already been extensively characterized in batch reactors.^[5,12] Moreover, **1b** has the potential to be used as a precursor for anticonvulsant drugs.^[31] The setup has been optimized with a face-centered composite (FCCD) design-of-experiments (DoE) approach^[32] to identify the best operating conditions in the flow setup to achieve high product formation and specific activity of the cells. This strategy was also chosen to speed up the optimization phase while minimizing waste and saving time and resources.^[33] The selected parameters for the DoE were flow rate and light intensity, the cell density was then further investigated at the optimal process conditions identified in the DoE. Moreover, the ene-reductions of two additional substrates, cyclohexenone (**2a**) and cyclopentenone (**3a**), were carried out to test the activity of recombinant Syn harboring YqjM for other substrates and compare the results obtained in batch. These compounds are particularly interesting as they can be further oxidized to produce monomers for interesting biopolymers, such as polylactones.^[34] The setup was further tested for two promoters, the partially light-inducible P_{epc} and the light-inducible P_{psbA2} , which have been presented in previous works^[5,12] to investigate the effect of the enzyme concentration inside the cells on the overall activity. Finally, a comparison among different reactor types and designs, namely batch, continuous stirred tank reactor (CSTR), coil, and the previously described BCR has been outlined, in terms of achieved productivity and STY at the optimal process conditions.

Results and Discussion

All experiments were carried out in the setup shown in Scheme 1a. It comprises a coil reactor made of a food-grade transparent PVC tube (ID 2 mm, length 1.5 m, 4.7 mL internal volume) wrapped in a helical shape around a fluorescent tube lamp (from OSRAM, for the technical details see the Supporting Information). The tubes are held in place using in-house-designed and 3D-printed tube holders (see the Supporting Information for more information). By changing the distance of the holders from the lamp, it is possible to regulate the light intensity irradiated to the coil. The reaction solution, which included the cyanobacterial cell suspension and the substrate, was pumped through the reactor in recycle mode via a peristaltic pump (ISMATEC® Reglo digital) equipped with a silicon tube for fluid delivery. No CO₂ was pumped into the system, since it is not required in the biotransformation and the cells proved to preserve their metabolic functions also under lower CO₂ availability.^[5] The inlet tube is connected to the coil reactor on one side via standard Luer-lock connectors, and on the other side it is connected to the reaction solution. The reactor was operated at room temperature, to keep the setup compact and reduce energy requirements from heating devices, as well as to avoid overheating of pumps and electrical devices over long operating times. Timely measurements of the temperature at the reactor outlet with a PT100 temperature sensor proved that the temperature did not rise above 25 °C during operation, therefore no cooling system was implemented as the

lamp heat dissipation was deemed negligible. At the inlet, middle and outlet of the reactors, flow-through cells equipped with Luer-lock connectors are also present for attaching additional sensors if needed.

The setup was tested for the model reaction shown in Scheme 1b, where the *Synechocystis* cells with the P_{epc} promoter for the expression of YqjM were used as biocatalyst. The reaction has already been extensively investigated on a 1 mL scale,^[5,12] for which after testing the reaction performance for a cell density between 0.48 and 2.4 g_{CDW}L⁻¹ [optical density (OD₇₅₀) between 2 and 10], the optimal conditions were found for a cell density of 2.4 with 10 mM as a starting material concentration. Especially in batch, it was found that the cell concentration greatly influenced the reaction rate, with densities higher than 1.8 g_{CDW}L⁻¹ resulting in unchanged reaction rate and lower specific activity. The same trend was set to be investigated in flow by expanding the investigated cell densities to the range between 0.48 and 4.8 g_{CDW}L⁻¹. However, some additional process parameters needed to be determined beforehand to translate the reaction from batch to flow, namely flow rate and light intensity. The flow rate is of crucial importance, since it regulates the residence time in the reactor and, in the case of photocatalytic reactions, the irradiation time, which can affect the reaction rate. In fact, if the irradiation time is too long, it can cause oxidative stress inside the cells. On the other hand, if it is too short, the cells will not get enough light to fuel photosynthesis and the subsequent NADPH regeneration. Therefore, the preliminary experiments were organized systematically with a DoE approach to increase the knowledge of the reaction and reduce the experimental time while minimizing waste. The two factors, namely light intensity and flow rate were tested at three levels according to a faced central composite design approach. For the light intensity, a low level of 150 μmol m⁻² s⁻¹ was chosen, as it was previously used in batch, and two other levels were added (300 and 450 μmol m⁻² s⁻¹) to screen the effect of light on a larger area. For the flow rate, the levels 0.2, 0.8, and 1.4 mL min⁻¹ (corresponding to residence times of 23.55, 5.88, and 3.36 min, respectively) were chosen, both due to the structural limits of the pump (0.2 mL min⁻¹ being the lowest operating point) and because a flow rate higher than 1.4 would not allow enough residence time for the reaction solution to be irradiated by the light. This choice of DoE yielded 9 possible combinations, which were all repeated in duplicates, except for the central point, which was replicated in independent biological triplicates, for a total of 19 runs. All experiments were carried out using 10 mM of **1a** and a cell density of 2.4 g_{CDW}L⁻¹ (OD₇₅₀ = 10), chosen as the middle value of the cell density range to be investigated later on. The different combinations for each run and the subsequent results are summarized in Table 1. For each run, the initial reaction rate and the specific activity were determined as response parameters. The initial reaction rate is calculated from the slope of the linear part of the progression curve, where the conversion of **1a** is below 20% and is given in mm h⁻¹. The specific activity (SA) has been calculated as follows [Eq. (1)]:

Table 1. Summary of the results obtained for the preliminary optimization tests. The experiments were carried out at a cell density of $2.4 \text{ g}_{\text{CDW}} \text{ L}^{-1}$ ($\text{OD}_{750} = 10$) and with a starting concentration of 10 mM **1a**. The specific activity was measured by taking the linear part of the progress curve, typically after 15 min from the reaction start. All experiments were replicated in duplicates, except for the center point, which was repeated in independent biological triplicates.

Run	Light intensity [$\mu\text{mol m}^{-2} \text{ s}^{-1}$]	Flow rate [mL min^{-1}]	Initial reaction rate [mM h^{-1}]	Specific activity [$\text{U g}_{\text{CDW}}^{-1}$]
1	450	1.4	2.8 ± 0.3	19.7 ± 1.9
2	150	0.2	2.0 ± 0.4	14.4 ± 2.7
3	300	0.8	6.0 ± 0.3	42.6 ± 1.8
4	450	0.2	3.3 ± 0.3	23.1 ± 1.4
5	150	1.4	2.3 ± 0.2	16.6 ± 1.2
6	300	0.2	5.3 ± 0.3	38.1 ± 2.4
7	300	1.4	4.1 ± 0.4	28.8 ± 3.1
8	450	0.8	3.2 ± 0.1	22.8 ± 0.4
9	150	0.8	3.3 ± 0.4	23.3 ± 2.8

$$\text{SA} = \frac{r_{1b}}{g_{\text{CDW}}} \quad (1)$$

Where r_{1b} is the initial formation rate of **1b** [$\mu\text{mol L}^{-1} \text{ min}^{-1}$, also indicated as U] and g_{CDW} is the cell density [g L^{-1}]. The obtained results showed how shifting towards the middle range for both the flow rate and light intensity gave the best results in terms of reaction rate and specific activity. This proved that optimal irradiation is achieved at around $300 \mu\text{mol m}^{-2} \text{ s}^{-1}$ (within the investigated space) and a flow rate of 0.8 mL min^{-1} . The use of a lower flow rate did not prove optimal, most probably due to prolonged residence and irradiation time and lower mixing in the reaction solution, while the use of a higher flow rate also proved inefficient since the residence time was in this case too low. Also, increasing the light intensity improved the reaction rate only until $300 \mu\text{mol m}^{-2} \text{ s}^{-1}$, then at $450 \mu\text{mol m}^{-2} \text{ s}^{-1}$, the reaction proceeded again at half the rate achieved at the optimum. Limited change was noticed among the runs with different flow rates and highest light intensity,

indicating that over irradiation and subsequent light-induced stress of the cells is the dominant effect independently from the residence time. Therefore, it does not make sense to use a more powerful lamp or decrease the distance to the light source.

The DoE results have been fitted according to a second order polynomial function [Eq. (2)]:

$$f(x, y) = a + bx + cy + dxy + ex^2 + fx^2 \quad (2)$$

where $f(x, y)$ indicates the response factor, in this case the product formation rate, x represents the flow rate, and y the light intensity. The regression parameters ($a-f$) were determined with a MATLAB script using the nonlinear least-square fitting function. The resulting model was then plotted as both a surface and contour plot, as shown in Figure 1. The results followed a Gaussian-shaped distribution with a good fitting score ($R^2 > 0.94$).

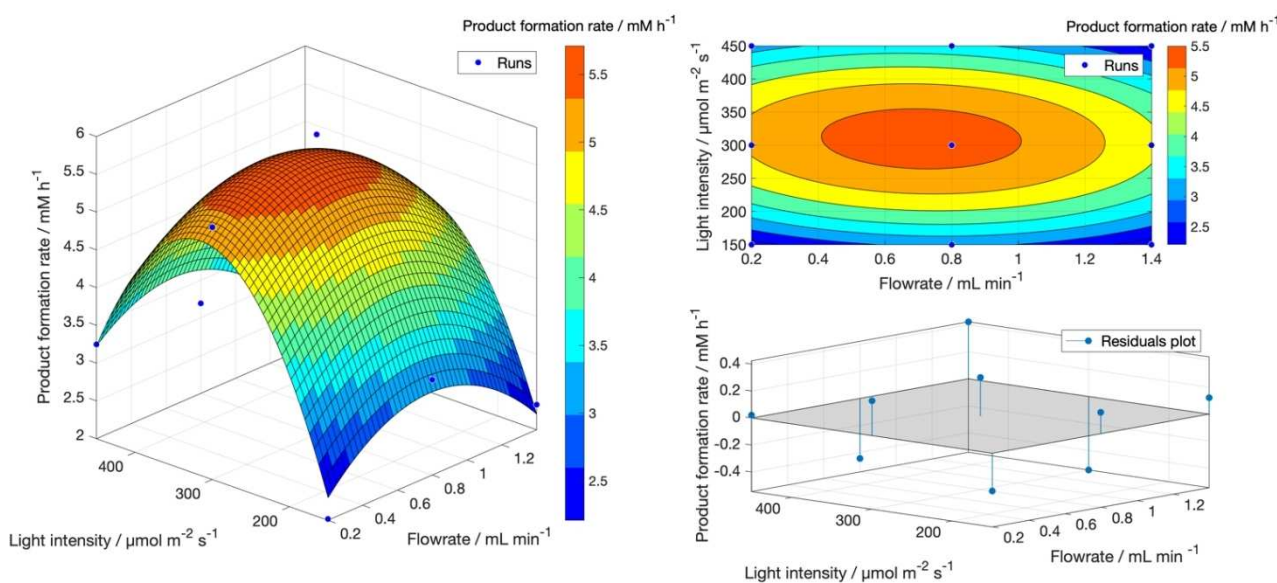


Figure 1. Response surface model for the preliminary investigation of the process parameters. Results evaluated in MATLAB® using the least square fitting function. As shown by the residuals plot, the deviation from the predicted to the actual value for the product formation rate is close to 0, indicating that the obtained model can represent the data with satisfactory accuracy.

After determining the necessary process parameters for the flow setup, the effect of the cell density on the reaction rate was investigated. For this purpose, the following cell densities were tested: 0.48, 1.2, 2.4, 3.6, and 4.8 $\text{g}_{\text{CDW}}\text{L}^{-1}$ (corresponding to $\approx \text{OD}_{750} = 2, 5, 10, 15, 20$). Each point was evaluated at the optimal operating conditions found in the previous step (0.8 mLmin^{-1} , 300 $\mu\text{mol}\text{m}^{-2}\text{s}^{-1}$, and 10 mM of substrate). The results summarized in Figure 2a,b show that the initial product formation rate increased 15-fold in the range from 0.48 until 3.6 $\text{g}_{\text{CDW}}\text{L}^{-1}$ (i.e., 0.84 to 13 mMh^{-1}). The specific activity was increased two-folds at 3.6 $\text{g}_{\text{CDW}}\text{L}^{-1}$ compared to 0.48 $\text{g}_{\text{CDW}}\text{L}^{-1}$ (60.7 $\text{U}\text{g}_{\text{CDW}}^{-1}$ compared to 33 $\text{U}\text{g}_{\text{CDW}}^{-1}$). Then between 3.6 and 4.8 $\text{g}_{\text{CDW}}\text{L}^{-1}$ no change in activity and only a limited increase in the product formation rate is recorded (60.7 $\text{U}\text{g}_{\text{CDW}}^{-1}$ at 3.6 and 58.7 $\text{U}\text{g}_{\text{CDW}}^{-1}$ at 4.8 $\text{g}_{\text{CDW}}\text{L}^{-1}$), indicating a limit due to self-shading effects. Therefore, a density of 3.6 $\text{g}_{\text{CDW}}\text{L}^{-1}$ resulted in the optimum, in contrast with what was obtained previously in batch,^[5] where the optimum activity was detected at 1.2 $\text{g}_{\text{CDW}}\text{L}^{-1}$ and the highest product formation rate at 2.4 $\text{g}_{\text{CDW}}\text{L}^{-1}$. The reason for this result could be that in flow, due to the improved light distribution and the decreased light diffusion path, the self-shading effect of the cells is dampened, and the cell density can be increased to higher levels without losing specific activity. Therefore, the

setup can be operated with a cell density of 3.6 $\text{g}_{\text{CDW}}\text{L}^{-1}$ without obvious negative effects on productivity caused by self-shading. However, the product formation rate is very low for 0.48 $\text{g}_{\text{CDW}}\text{L}^{-1}$ (around 1 mMh^{-1}) compared to what was obtained in batch (2.5 mMh^{-1}). Nevertheless, at the optimum conditions achieved in this work (i.e., 3.6 $\text{g}_{\text{CDW}}\text{L}^{-1}$), a 1.4-fold increase in initial reaction rate was observed as compared to the optimal conditions in batch, with cells cultivated at the same conditions as in our work.^[5] Furthermore, we would like to highlight that the specific activity achieved at these conditions in the coil was also higher than in the batch from reference,^[5] although it was measured to be higher at standard cultivation conditions in a previous work.^[12]

Compared to whole-cell biotransformations in the BCR at the optimal cell concentration of 2.4 $\text{g}_{\text{CDW}}\text{L}^{-1}$, a 1.6-fold increase was observed in our continuous set-up.^[5] Moreover, a 2.5-fold higher initial reaction rate was recorded at the optimal conditions of this work. Complete conversion was also achieved after 90 min using the coil reactor compared to 4–5 h using the BCR. However, it is noteworthy to mention that the experiments in batch and BCR were conducted at 30 °C, not at room temperature as in this work.

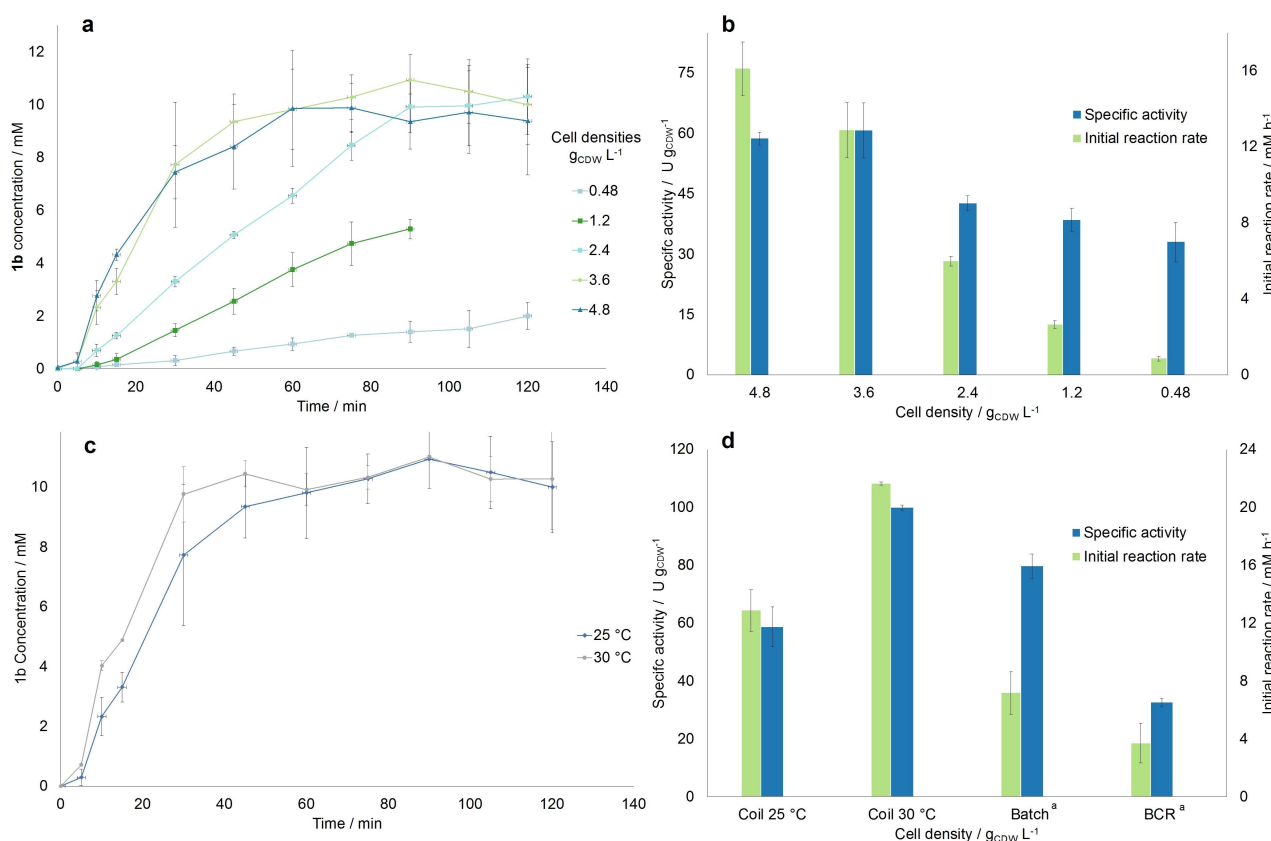


Figure 2. Summary of the results of the investigation of the effect of the cell OD_{750} on the model reaction rate. (a) Progression curve determined for the 5 investigated OD_{750} including the determined standard deviation. (b) Specific activity and product formation rate determined for each OD_{750} , calculated with the slope of the first 15 min of the progression curve. (c) Comparison of the progression curves for the experiments carried out in the coil reactor both at room temperature and at 30 °C, both at optimal operating conditions. (d) Comparison of the specific activities achieved at best reaction conditions for different reactor geometries. [a] The results in the batch and BCR were retrieved from Ref. [5]. For all figures, error bars correspond to standard deviations from at least three independent biological replicates.

To fairly compare the performance of these reactors with that of the coil reactor, the reaction was conducted at the optimal operating conditions of this work and at 30 °C, as this was the temperature used in previous works. Since the setup could not be inserted in an incubator, the coil reactor was placed in a temperature-controlled room set to 28 °C. The flask containing the reaction solution was further placed in a water bath heated to 30 °C, in order to achieve the desired temperature. As shown in Figure 2c,d, the temperature increase had a positive effect on the initial reaction rate and specific activity, which were estimated to be 21.5 mm h⁻¹ and 99.8 U g_{CDW}⁻¹ (corresponding to 9.2 U mg_{chla}⁻¹), respectively around 1.6 times higher compared to the room temperature values (13 mm h⁻¹ and 60.7 U g_{CDW}⁻¹, corresponding to 5.2 U mg_{chla}⁻¹). Moreover, steady-state conversion was achieved at around 30 min

compared to the 60 min needed at room temperature. The obtained value for the initial reaction rate in the coil at 30 °C was also the highest recorded for Syn::P_{cpc} yqjM and is around 2.8 and 5.8 times greater than the optimal values obtained in the 1 mL batch and the BCR, respectively.^[5] This confirmed the trend already seen at 25 °C that the flow reactor does improve the reaction performance compared to batch processes.

We further tested other substrates under the same conditions to validate our results. Cyclohexenone (2a) and cyclopentenone (3a) were chosen since they were tested in previous works^[12,14] for the YqjM catalyzed reduction to cyclohexanone (2b) and cyclopentanone (3b), respectively. The reactions were carried out at the optimal process parameters investigated before, except for the cell density that was selected to be 2.4 g_{CDW}L⁻¹ to take the middle value of the investigated range and compare the results with the previous findings in batch. The results are reported in Figure 3. As visible from the graph, the activity and formation rate obtained with 2a was noticeable (≈ 25 U g_{CDW}⁻¹, corresponding to 1.8 U mg_{chla}⁻¹), however for 3a the activity was very low (< 5 U g_{CDW}⁻¹, corresponding to 0.29 U mg_{chla}⁻¹). This confirmed the trend found in batch,^[14] with 1a being the best substrate in terms of activity, despite maleimide complexes being toxic to the cell metabolism.^[12] Nevertheless, no formation of the undesired side products, cyclohexanol and cyclopentanol, due to ketoreduction catalyzed by endogenous alcohol dehydrogenase were measured, compared to what was observed in batch,^[12] most probably due to the improved mixing properties inside the coil reactor deriving from its small internal dimensions.

An additional test was conducted to compare the effect on the activity when using two different promoters for the expression of YqjM, namely the partially light-inducible P_{cpc} and the light-inducible P_{psbA2}. The use of the two promoters was compared at the optimal process conditions for both 2.4 and 3.6 g_{CDW}L⁻¹. As shown in Figure 4, for 2.4 g_{CDW}L⁻¹, the reaction reached completion within the 2 h of experiment for both cell

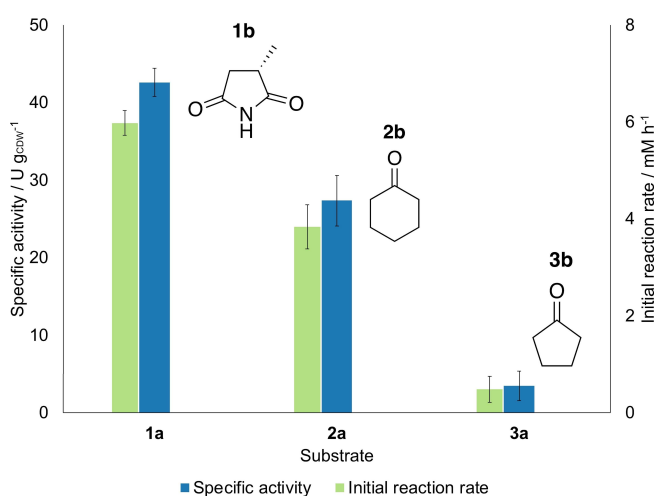


Figure 3. Reduction of various substrates catalyzed by Syn::P_{cpc} yqjM. All experiments were carried out with 0.8 mL min⁻¹, 300 μmol m⁻² s⁻¹, 2.4 g_{CDW}L⁻¹ and 10 mM of substrate. Error bars correspond to standard deviations from at least three biological replicates.

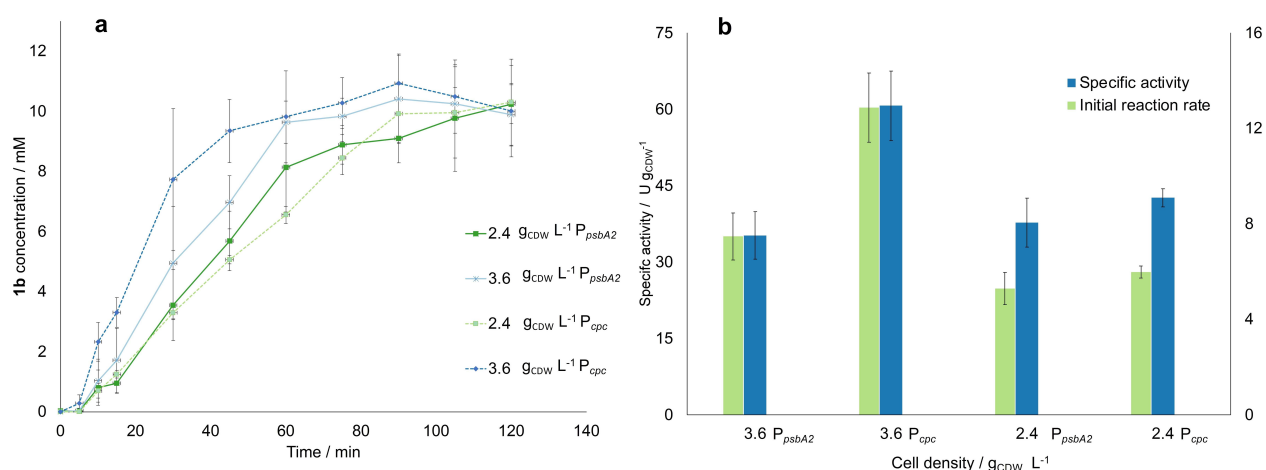


Figure 4. Summary of the results for the investigation of the two different promoters P_{psbA2} and P_{cpc}. (a) Progression curves estimated at the optimal operating conditions and a cell density of for 2.4 and 3.6 g_{CDW}L⁻¹ for both investigated promoters, estimated with gas chromatography with flame ionization detector (GC-FID). (b) Estimated specific activity and initial reaction rate. For both figures, error bars correspond to standard deviations from at least three independent biological replicates.

types. However, the experiment at $2.4 \text{ g}_{\text{CDW}} \text{ L}^{-1}$ for P_{cpc} was 1.2 times faster. This result is in line with what was obtained in previous works,^[5,12] where P_{cpc} proved to be a stronger promoter than P_{psbA2} . The difference in product formation rate and specific activity is even more marked when comparing the results for $3.6 \text{ g}_{\text{CDW}} \text{ L}^{-1}$. In this case, the reaction rate was 1.8 times lower when using P_{psbA2} . This indicates that the cells are even more negatively affected by the lower light penetration depth in the experiment when using P_{psbA2} , which is not the case for P_{cpc} . However, since this cell density was not investigated in batch, we cannot draw further conclusions. We can only suggest, as done in a previous work,^[12] that whole-cell biotransformations in *Synechocystis* could be limited by several factors other than the intracellular enzyme concentration, such as quality of the light distribution. Nevertheless, promoter engineering proved to work in the coil reactor as well, since there was a noticeable improvement in activity when using $\text{Syn}::P_{\text{cpc}}$ over $\text{Syn}::P_{\text{psbA2}}$.

As a proof of concept for the validity of the presented setup, we set out to compare the performance of different reactors at the investigated optimal conditions identified in this work. Therefore, the results obtained in the coil reactor were compared to a batch and a CSTR experiment carried out with a cell density of $3.6 \text{ g}_{\text{CDW}} \text{ L}^{-1}$, a light intensity of $300 \mu\text{mol m}^{-2} \text{ s}^{-1}$,

10 mM of **1a** at room temperature. Batch reactions were carried out in a 10 mL flask filled with the same volume as the internal volume of the coil (4.71 mL). The CSTR was carried out by circulating the reaction solution (15 mL as in the coil experiment) with 0.8 mL min^{-1} through a stirred tank filled up to the internal volume of 4.71 mL (see the Supporting Information for the setup scheme). The reaction progress curves are reported in Figure 5a. As expected, the initial reaction rate and specific activity are greatly affected by different reactor geometries, with a starting value of 3.88 mM h^{-1} in batch followed by a 36% increase to 6.05 mM h^{-1} to a further 53% increase to 13 mM h^{-1} in the coil reactor. This trend is also mirrored in the specific activity, proving that the coil reactor allows for better light distribution and lower self-shadowing of the cells. As visible in Table 2, the coil reactor has a 10-fold higher surface area/volume ratio. The acquired results were further compared to those obtained on both a 1 mL scale and in the BCR, both investigated for the same reaction in previous works.^[5,12] Even though a cell density of $3.6 \text{ g}_{\text{CDW}} \text{ L}^{-1}$ had not been investigated before, it is still possible to make some considerations on the productivity at optimal operating conditions, $2.4 \text{ g}_{\text{CDW}} \text{ L}^{-1}$, at which the highest initial reaction rate was recorded for both reactor types.

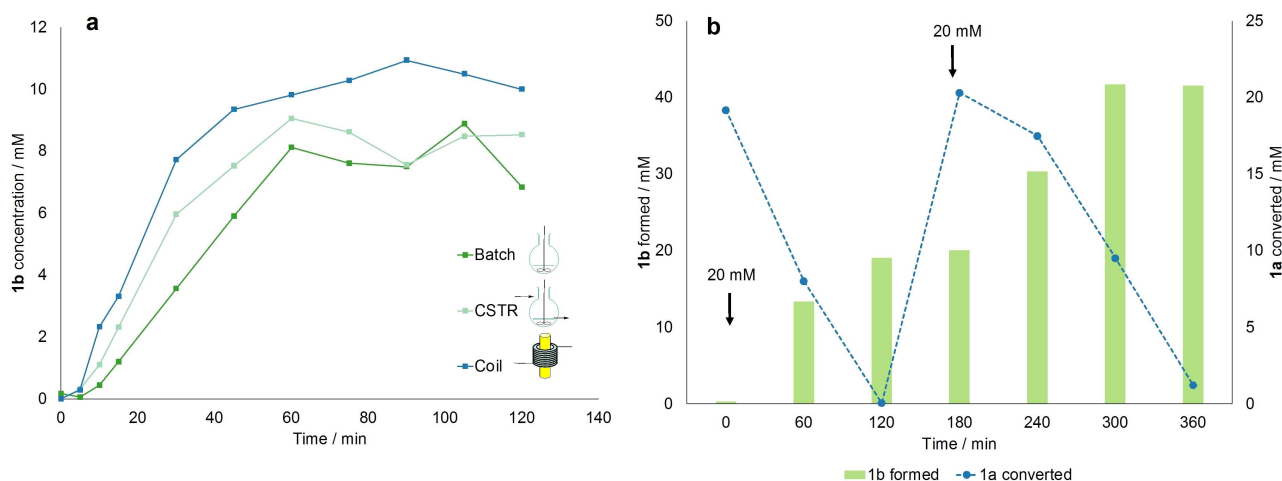


Figure 5. (a) Comparison of the progress curves for the experiments carried out in different reactor geometries. Starting concentration of **1a** 10 mM, $300 \mu\text{mol m}^{-2} \text{ s}^{-1}$, and $3.6 \text{ g}_{\text{CDW}} \text{ L}^{-1}$ cell density. Single measurements. (b) Amount of **1a** converted (blue line) and **1b** formed (green bars) measured over 6 h during a double substrate feeding experiment, where 20 mM of **1a** are initially supplied to the system and subsequently fed again after 3 h. Single measurements.

Table 2. Summary of the comparison of different reactor geometries used in this work.

Reactor type	Reactor volume [cm ³]	Reactor surface [cm ²]	Surface area/volume [m ² m ⁻³]	Initial reaction rate [mM h ⁻¹]	Specific activity [U g _{CDW} ⁻¹]	STY [g L ⁻¹ h ⁻¹]
batch (5 mL scale)	4.7	11.2	225	3.8	18.3	0.4
CSTR	22.5	38.5	171	6.0	28.5	4.1
coil (25 °C)	4.7	94.3	2000	13.0	60.7	8.5
coil (30 °C)				21.5	99.8	14.4
batch ^[a] (1 mL scale)	1.0	3.4	345	7.5	50.0	0.6
BCR ^[a]	200	160	80 ^[b]	3.7	32.5	0.3

[a] The values for the 1 mL batch and the BCR after cultivation under the same conditions were taken from Ref. [5]. [b] Calculated from the dimensions of the BCR but not considered for comparison, since the actual irradiated surface area is higher for this reactor due to the internal illumination principle adopted, but it could not be determined.

To extend the reactor comparison in terms of volumetric productivity, the STY was used as a parameter to compare across the different reactor geometries and was calculated as follows [Eq. (3)]:

$$\text{STY} = \frac{g}{V_R \times t_R} \quad (3)$$

Where g is the amount of **1b** formed in one residence time, V_R is the internal reactor volume [L], and t_R is the reaction time for batch and the residence time in case of flow operation [h]. As visible from Table 2, the presented continuous flow reactors have a higher STY than the batch setups. The CSTR showed an STY of $4.1 \text{ g L}^{-1} \text{ h}^{-1}$, while the coil had an STY of more than double that, namely $8.5 \text{ g L}^{-1} \text{ h}^{-1}$, representing a 22-fold increase in STY compared to batch with the same internal volume as the coil. Such an increase can be attributed to the higher surface area in the coil reactor. This results in better and more uniform light distribution and reduced light diffusion path from the light source, as well as improved mixing properties, which has proven to enhance mass transfer inside the reactor and boost the reaction rate. Compared to the results from literature in the 1 mL batches, the coil reactor outperformed these results at both 25 and 30 °C, with an STY up to 25-fold higher than in batch (0.56 against $14.4 \text{ g L}^{-1} \text{ h}^{-1}$). Regarding the BCR, despite the short light diffusion path and improved biocatalyst loading due to the internal illumination principle, the reactor still suffered from significantly lower reaction rates and productivity than the presented continuous approach (i.e., 0.22 against $14.4 \text{ g L}^{-1} \text{ h}^{-1}$ for the coil at 30 °C). It is a valid alternative for scaling up photobiocatalytic reactions; however, bigger reactors could suffer from inefficient mixing and uneven light distribution, while in a coil reactor it is easier to achieve a better light distribution due to the improved surface area. Moreover, it is essential to consider the oxygen accumulation in the reactor, which needs to be controlled during scale-up to avoid photoinhibition.^[35] This can be particularly high in large-scale batch reactors but can be more easily mitigated in smaller-volume reactors, such as continuous-flow micro- and meso-reactors, without sacrificing productivity.

A final multiple feeding experiment was carried out and recorded to test the cells' viability over longer operating times, as done in a previous work.^[5] The experiment was carried out at the optimal operating conditions, and at room temperature to avoid overheating of the pump over long operating times in the temperature-controlled room. The results are reported in Figure 5b. The system was first provided with 20 mM of **1a**, then the reaction proceeded to completion in the first 2 h, with an initial reaction rate of 14 mM h^{-1} . After 3 h, 20 mM of **1a** were again fed to the system, and the reaction proceeded slower (initial reaction rate 5.55 mM h^{-1}), but still almost all of **1a** was converted after 3 h. Using this approach, 40 mM (corresponding to 65 mg, not isolated) of **1b** were produced in 6 h, with an STY of $59.2 \text{ g L}^{-1} \text{ h}^{-1}$. The product was further isolated as described in the Supporting Information: 50.6 mg were obtained (77% yield) with outstanding optical purity [$> 99\%$ enantiomeric excess (ee)] via extraction and evaporation,

without need for additional purification steps. Compared to the same experiment carried out in the BCR reactor, the coil proved once more to be a more efficient reactor, since full conversion of the total 40 mM of **1a** was achieved within 6 h, while in a BCR 22 h were necessary. The turnover number (TON) was further calculated to compare the two setups [Eq. (4)]:

$$\text{TON} = \frac{g_{1b}}{g_{CDW}} \quad (4)$$

where g_{1b} is the amount of **1b** [g] formed after 6 h (not isolated), and g_{CDW} is the amount of whole-cells used in the reactor [g]. The TON resulted to be $1.2 g_{1b} g_{CDW}^{-1}$ for the coil reactor, which was 25% higher to the value obtained for the BCR ($0.92 g_{1b} g_{CDW}^{-1}$).

Due to the improved reaction rates, the presented process proved to be the most time- and cost-effective solution to the continuous reduction of **1a** to **1b**. Moreover, this setup could be the starting point for increasing the production of **1b** by following the numbering-up approach. By using more coil reaction units in parallel, it would be possible to linearly increase the production of **1b** without sacrificing the optimal light intensity distribution, mixing properties, and ease of heat management achieved in the single reaction unit. This strategy could be additionally coupled with a scaling-out approach, meaning running the process over longer times.

Lastly, to assess the sustainability of the process, the E factor was chosen as a green metric and calculated for the multiple feeding experiment, both in our coil reactor and in the BCR. Since the process was carried out on a lab scale, the simple E factor (sE) formula was used, as suggested in literature [Eq. (5)].^[36]

$$sE = \frac{\sum m(\text{raw materials}) + \sum m(\mathbf{1a}) - m(\mathbf{1b})}{m(\mathbf{1b})} \quad (5)$$

where the raw materials include the cells dry weight and the buffer ingredients, all reported in g (for more details on the calculations, see the Supporting Information). The resulting value for the coil was 1.7, which was 2.3 times lower than the value estimated for the process carried out for the same operating time in the BCR (3.9). This result hints that the presented setup has the potential of being more sustainable, due to the lower amount of waste produced. However, it is only a rough estimation, and would need to be re-evaluated when switching from lab to pilot plant scale, by taking into account the water consumption and other production steps (e.g., Syn cultivation) for an overall environmental impact assessment.

To conclude, our results show that photobiotransformations within cyanobacteria in continuous flow have the potential of being sustainable alternatives for the production of fine chemicals. However, light distribution and harvesting are major limiting factors for the scale-up of such processes. Identifying the optimal light intensity range as well as choosing an appropriate reactor geometry with high S/V is essential in the early stages of process development. Flow reactors with small internal dimensions and high S/V ($> 10^3$) are indeed a valid

choice to achieve uniform light distribution and lower light diffusion paths within the reactor, thereby reducing the occurrence of dark zones resulting in higher reaction rates and STY. In the specific case of biotransformations in whole-cells, the biocatalyst loading is also an essential parameter that needs improvement. We have demonstrated that the enhanced illumination in flow reactors can help overcome cell density limitations and self-shading effects. Therefore, it is possible to increase biocatalyst loading ($> 2.4 \text{ g}_{\text{CDW}} \text{ L}^{-1}$) and, as a consequence, to speed up the biocatalytic process. The temperature also played a role, since increasing it from 25 to 30 °C showed a great improvement in the productivity. Nevertheless, considering the energy effort of keeping the setup in a temperature-controlled room, as well as the risk of overheating valuable flow equipment (e.g., pumps), we believe that our approach with a room temperature setup is a more energy- and cost-efficient solution, which still provided faster reaction rates and outperformed the productivity achieved with batch processes.

Considering energy and resources demand, it is noteworthy to mention that the system was non-sterile, and the cells showed good compatibility with the silicon and PVC inner parts without need for autoclaving. This further proves the versatility and applicability of Syn as well as of the setup.

Due to its compact construction, flexibility, and high surface area/volume, we believe that the presented setup could be successfully used in the future to screen other photobiotransformations within recombinant *Synechocystis* cells on a lab scale. An interesting example would be oxyfunctionalizations, which have already been investigated in batch.^[16] Furthermore, the setup could be easily scaled up in the future following common continuous scale-up approaches such as scaling out, increasing the reactor length or flow rate, or using more units in parallel (numbering-up).^[21,37] The latter would be a promising solution to increase the production without having to re-optimize the critical process parameters and therefore without sacrificing the specific activity, which is currently the biggest issue for scaling-up photobiotransformations.^[5,30] The type of scale-up will depend mainly on the purpose and can be selected on a case-to-case basis; however, we believe the setup is flexible enough to be adapted to a plethora of photobiotransformations. Additionally, we further plan to exploit the great activity of *Synechocystis* sp. PCC 6803 in other reactor geometries, via investigating immobilization strategies for flow (multi-step) production of fine chemicals.

Conclusion

In this work, we demonstrated the application of a robust continuous coil reactor setup for improving the productivity of photobiocatalytic ene-reductions within recombinant cyanobacteria. The first step of process investigation was a design-of-experiments optimization to identify the optimal light intensity and flowrate, which were found at $300 \mu\text{mol m}^{-2} \text{ s}^{-1}$ and 0.8 mL min^{-1} . The cell density effect was further investigated, and it was proven that the biocatalyst loading could be increased up to 4.8 g L^{-1} without activity losses due to self-

shading. Moreover, at optimal conditions, the coil reactor gave, to our knowledge, the highest initial reaction rate ever recorded, achieving a value of 21.5 mm h^{-1} . To show the merits of the continuous setup, we have compared its performance to the results obtained in a batch and continuous stirred tank reactor. Here, both continuous reactor configurations could reach higher space-time-yields (STYs) compared to batch. The coil reactor could also outperform the productivity achieved in batch and bubble column reactor: there, a STY of $0.22 \text{ g L}^{-1} \text{ h}^{-1}$ was achieved, against the $14.4 \text{ g L}^{-1} \text{ h}^{-1}$ achieved at 30 °C in this work, marking a 60-fold increase in productivity. The results demonstrate that the utilization of flow reactors can help improving the illumination efficiency, therefore allowing for more sustainable and easily scalable photobiotransformations.

Experimental Section

Chemicals

The substrate **1a** was synthesized according to the literature procedure.^[14] The product **1b** was isolated from the reaction mixture as described in a previous work.^[5] The nuclear magnetic resonance (NMR) spectra of both substances are available in the Supporting Information. All other chemicals were purchased from Sigma Aldrich or TCI Chemicals (unless otherwise stated) and used as received.

Strains

Synechocystis sp. PCC 6803 harboring the *YqjM* gene from *Bacillus subtilis* was constructed by homologous recombination targeting the gene locus *slr0168*. The gene was integrated under the control of light-inducible promoters, P_{cpc} and P_{psbA2} as previously described.^[5,12]

Synechocystis cultivation conditions

Synechocystis seed cultures were cultivated in liquid BG-11 (pH 8) supplemented with $50 \mu\text{g mL}^{-1}$ kanamycin as selectable marker. The flask was kept in a growth chamber (SWGC-1000, WISD lab instruments) maintained at 30 °C, 50% relative humidity, and illuminated with white fluorescent lamps delivering a light intensity of $40\text{--}60 \mu\text{mol}_{\text{photons}} \text{ m}^{-2} \text{ s}^{-1}$. Cultures were placed on vertical rotary shakers fitted in the growth chambers under ambient CO_2 and harvested by centrifugation after reaching an $\text{OD}_{750} = 1\text{--}2$. After re-suspending in fresh BG-11, the cells were inoculated in gas washing tubes ($V = 200 \text{ mL}$) as previously described.^[5] The tubes were placed in an aquarium maintained at 30 °C and illuminated with six fluorescent lamps delivering a light intensity of $200\text{--}250 \mu\text{mol}_{\text{photons}} \text{ m}^{-2} \text{ s}^{-1}$. Mixing and aeration was provided by bubbling using an air pump (Boyu S-4000B pump). The conditions were maintained sterile by passing air through a $0.20 \mu\text{m}$ filter. A correlation of $2.4 \text{ g}_{\text{CDW}} \text{ L}^{-1}$ for an $\text{OD}_{750} = 10$ was utilized as reported previously.^[12]

Quantification of chlorophyll a content

The amount of chlorophyll *a* was estimated as described previously.^[12] Before each biotransformation, a $100 \mu\text{L}$ sample from the cell suspension with known OD_{750} was pelleted, resuspended in $100 \mu\text{L}$ double distilled water (ddH_2O) and $900 \mu\text{L}$ methanol was

added. The solution was vortexed and incubated in darkness for 10 min to extract chlorophyll *a*. After further centrifugation, the absorption at 665 nm was measured in an Avantes AvaLight-DS-DUV spectrometer, equipped with a deuterium lamp and a AvaSpec-ULS2048 detector. The amount of chlorophyll *a* was determined using the extinction coefficient $\epsilon = 78.74 \text{ L g}^{-1} \text{ cm}^{-1}$. From the chlorophyll content, it is also possible to cross-check the OD value, according to the correlation from literature.^[12]

Whole-cell biotransformations

After cultivation, cells were harvested by centrifugation upon reaching an $\text{OD}_{750} = 1\text{--}3$. The pellets were resuspended in BG-11 to obtain an $\text{OD}_{750} = 25\text{--}33$ and were subsequently diluted to the desired OD_{750} for the biotransformations. The reactions were carried out in a coil reactor, with a length of 1.5 m and 2 mm internal diameter, and an empty volume of 4.71 mL. The coil was wrapped around a neutral white fluorescent lamp from OSRAM, and the light intensity was adjusted by setting the distance of the tube from the lamp, according to the intensity value measured at the reactor wall by a LI-250 A light meter (LICOR Biosciences, Hamburg, Germany) equipped with a spherical micro quantum sensor US-SQS/L (Walz, Effeltrich, Germany). The starting solution had a total volume of 15 mL. Firstly, the cell suspension and an appropriate amount of BG-11 were added to achieve the desired OD_{750} , then the substrate was added from a 100 mM stock solution in BG-11 to achieve the final concentration of 10 mM in 15 mL volume. The reaction solution was inserted in a stirred flask and was recirculated through the reactor via an ISMATEC® Reglo digital peristaltic pump. Before each run, a sample of the reaction solution (100 μL) was taken to determine the chlorophyll content as described above. All reactions were carried out at room temperature unless stated otherwise. Samples (200 μL) were taken every 0, 5, 10, 15, and then every 15 min for a total of 2 h per run. The 0 sample was taken from the reaction solution; the subsequent samples were withdrawn from the outlet tube.

GC analysis

Each sample from the biotransformations was extracted with ethyl acetate (600 μL) for **1a** and **1b** or DCM (600 μL) for **2a,b** and **3a,b** containing 2 mM of *n*-decanol as internal standard. The organic phase was dried over anhydrous MgSO_4 and measured with GC-FID. GC analysis was performed with a Perkin Elmer Clarus 500 equipped with an Optima-5 MS capillary column (Machery-Nagel, 30.0 m \times 320 μm ID, 0.25 μm) with a flame ionization detector (FID). To determine the optical purity (enantiomeric excess, *ee*) of **1b**, samples were measured using a GC-FID system (GC-2030, Shimadzu, Japan) equipped with a chiral β -6TBDAC column. For details on the GC methods, see the Supporting Information.

Acknowledgements

A.V., R.K. and H.G.W. acknowledge the funding by the CATALOX (CATalytic mechanisms and AppLications of OXidoreductases) project, doc.fund program funded by the Austrian Science Fund (FWF, fund number doc.46). This project has received funding from the European Union's Horizon 2020 research and innovation program under the FET Open grant agreement 899576 (Futuroleaf).

Conflict of Interest

The authors declare no conflict of interest.

Data Availability Statement

The data that support the findings of this study are available from the corresponding author upon reasonable request.

Keywords: biocatalysis · continuous flow · cyanobacteria · photobiocatalysis · photosynthesis

- [1] J. D. Williams, C. O. Kappe, *Curr. Opin. Green Sustain. Chem.* **2020**, *25*, 100351.
- [2] L. Buglioni, F. Raymenants, A. Slattery, S. D. A. Zondag, T. Noël, *Chem. Rev.* **2022**, *122*, 2752–2906.
- [3] K. Faber, *Biotransformations in Organic Chemistry*, Springer International Publishing, **2018**.
- [4] J. M. Woodley, *Appl. Microbiol. Biotechnol.* **2019**, *103*, 4733–4739.
- [5] M. Hobisch, J. Spasic, L. Malihan-Yap, G. D. Barone, K. Castiglione, P. Tamagnini, S. Kara, R. Kourist, *ChemSusChem* **2021**, *14*, 3219–3225.
- [6] P. T. Anastas, J. C. Warner, *Green Chemistry: Theory and Practice*, Oxford University Press, Oxford, **1998**.
- [7] L. Schmermund, V. Jurkaš, F. F. Özgen, G. D. Barone, H. C. Büchschütz, C. K. Winkler, S. Schmidt, R. Kourist, W. Kroutil, *ACS Catal.* **2019**, *9*, 4115–4144.
- [8] F. F. Özgen, M. E. Runda, S. Schmidt, *ChemBioChem* **2021**, *22*, 790–806.
- [9] C. J. Seel, T. Gulder, *ChemBioChem* **2019**, *20*, 1871–1897.
- [10] K. Buchholz, V. Kasche, U. T. Bornscheuer, *Biocatalysts and Enzyme Technology*, Wiley-VCH Verlag & Co. KGaA, **2012**.
- [11] A. T. Martínez, F. J. Ruiz-Dueñas, S. Camarero, A. Serrano, D. Linde, H. Lund et al., *Biotechnol. Adv.* **2017**, *35*, 815–831.
- [12] L. Assil-Companiononi, H. C. Büchschütz, D. Solymosi, N. G. Dyczmons-Nowaczyk, K. K. F. Bauer, S. Wallner, P. Macheroux, Y. Allahverdiyeva, M. M. Nowaczyk, R. Kourist, *ACS Catal.* **2020**, *10*, 11864–11877.
- [13] Y. Ni, D. Holtmann, F. Hollmann, *ChemCatChem* **2014**, *6*, 930–943.
- [14] K. Köninger, Á. Gómez Baraibar, C. Mügge, C. E. Paul, F. Hollmann, M. M. Nowaczyk, R. Kourist, Á. Gómez Baraibar, C. Mügge, C. E. Paul, F. Hollmann, M. M. Nowaczyk, R. Kourist, *Angew. Chem. Int. Ed.* **2016**, *55*, 5582–5585; *Angew. Chem.* **2016**, *128*, 5672–5675.
- [15] S. Böhmer, K. Köninger, Á. Gómez-Baraibar, S. Bojarra, C. Mügge, S. Schmidt, M. M. Nowaczyk, R. Kourist, *Catalysts* **2017**, *7*, 240.
- [16] E. Erdem, L. Malihan-Yap, L. Assil-Companiononi, H. Grimm, G. D. Barone, C. Serveau-Avesque, A. Amouric, K. Duquesne, V. de Berardinis, Y. Allahverdiyeva, V. Alphand, R. Kourist, *ACS Catal.* **2021**, *66*–72.
- [17] J. Jodlbauer, T. Rohr, O. Spadiut, M. D. Mihovilovic, F. Rudroff, *Trends Biotechnol.* **2021**, *39*, 875–889.
- [18] S. N. Chanquia, A. Valotta, H. Gruber-Woelfler, S. Kara, *Front. Catal.* **2022**, *1*, 816538.
- [19] Y. Su, N. J. W. Straathof, V. Hessel, T. Noël, *Chem. Eur. J.* **2014**, *20*, 10562–10589.
- [20] D. Cambié, C. Bottecchia, N. J. W. Straathof, V. Hessel, T. Noël, *Chem. Rev.* **2016**, *116*, 10276–10341.
- [21] C. Sambagiato, T. Noël, *Trends Chem.* **2020**, *2*, 92–106.
- [22] P. De Santis, L. E. Meyer, S. Kara, *React. Chem. Eng.* **2020**, *5*, 2155–2184.
- [23] A. I. Benítez-Mateos, M. L. Contente, D. Roura Padrosa, F. Paradisi, *React. Chem. Eng.* **2021**, *6*, 599–611.
- [24] Y. Zhu, Q. Chen, L. Shao, Y. Jia, X. Zhang, *React. Chem. Eng.* **2020**, *5*, 9–32.
- [25] E. J. S. Bras, V. Chu, J. P. Conde, P. Fernandes, *React. Chem. Eng.* **2021**, *6*, 815–827.
- [26] A. E. Case, S. Atsumi, *J. Biotechnol.* **2016**, *231*, 106–114.
- [27] P. Farrokh, M. Sheikhpour, A. Kasaean, H. Asadi, R. Bavandi, *Biotechnol. Prog.* **2019**, *35*, 10.1002/btpr.2835.
- [28] A. Hoschek, I. Heuschkel, A. Schmid, B. Bühler, R. Karande, K. Bühler, *Bioresour. Technol.* **2019**, *282*, 171–178.
- [29] I. Heuschkel, A. Hoschek, A. Schmid, B. Bühler, R. Karande, K. Bühler, *Data Br.* **2019**, *25*, 104059.

- [30] A. Tüllinghoff, M. B. Uhl, F. E. H. Nintzel, A. Schmid, B. Bühler, J. Toepel, *Front. Catal.* **2022**, 10.3389/fctls.2021.780474.
- [31] S. Rybka, J. Obniska, A. Rapacz, B. Filipek, K. Kamiński, *Arch. Pharm.* **2014**, *347*, 768–776.
- [32] G. E. P. Box, K. B. Wilson, *J. R. Stat. Soc. Ser. B* **1951**, *13*, 1–38.
- [33] P. M. Murray, F. Bellany, L. Benhamou, D. K. Bučar, A. B. Tabor, T. D. Sheppard, *Org. Biomol. Chem.* **2016**, *14*, 2373–2384.
- [34] D. Mondal, M. Griffith, S. S. Venkatraman, *Int. J. Polym. Mater. Polym. Biomater.* **2016**, *65*, 255–265.
- [35] A. Hoschek, A. Schmid, B. Bühler, *ChemCatChem* **2018**, *10*, 5366–5371.
- [36] R. A. Sheldon, *Green Chem.* **2017**, *19*, 18–43.
- [37] N. G. Anderson, *Org. Process Res. Dev.* **2012**, *16*, 852–869.

Manuscript received: August 1, 2022
Revised manuscript received: September 6, 2022
Accepted manuscript online: September 7, 2022
Version of record online: September 26, 2022